Effect of Moisture on the Field Dependence of Mobility for Gas-Phase Ions of Organophosphorus Compounds at Atmospheric Pressure with Field Asymmetric Ion Mobility Spectrometry

N. Krylova, E. Krylov, and G. A. Eiceman*

Department of Chemistry and Biochemistry, New Mexico State University, Las Cruces, New Mexico 88003

J. A. Stone

Department of Chemistry, Queens University, Kingston, Ontario, Canada

Received: September 20, 2002; In Final Form: February 26, 2003

The electric field dependence of the mobilities of gas-phase protonated monomers [$(MH^+(H_2O)_n$] and proton-bound dimers [$M_2H^+(H_2O)_n$] of organophosphorus compounds was determined at *E*/*N* values between 0 and 140 Td at ambient pressure in air with moisture between 0.1 and 15 000 ppm. Field dependence was described as $\alpha(E/N)$ and was obtained from the measurements of compensation voltage versus field amplitude in a planar high-field asymmetric waveform ion mobility spectrometer. The α function for protonated monomers to 140 Td was constant from 0.1 to 10 ppm moisture in air with onset of effect at ∼50 ppm. The value of α increased 2-fold from 100 to 1000 ppm at all *E*/*N* values. At moisture values between 1000 and 10 000 ppm, a 2-fold or more increase in $\alpha(E/N)$ was observed. In a model proposed here, field dependence for mobility through changes in collision cross sections is governed by the degree of solvation of the protonated molecule by neutral molecules. The process of ion declustering at high *E*/*N* values was consistent with the kinetics of ion−neutral collisional periods, and the duty cycle of the waveform applied to the drift tube. Water was the principal neutral above 50 ppm moisture in air, and nitrogen was proposed as the principal neutral below 50 ppm.

Introduction

Gas-phase ions in an electric field exhibit a velocity of drift that can be used to explore interactions between ions and neutrals of the supporting atmosphere.[1,2] The velocity of the ion drift (v_d) is defined as the product of electric field (*E*) and the mobility coefficient (*K*) when the ions dissipate, through collisions, whatever energy is acquired from the electric field between collisions. Under such conditions, the ions are regarded as thermalized and the mobility coefficient is independent of the electric field (i.e., $K = v_d/E$, $cm^2/(V\ s)$). This occurs for ambient pressure studies at electric fields, calculated as *E*/*N* values, of ≤30 Td and has been called the low field limit.[3] As the magnitude of *E*/*N* is increased above this limit, the mobility coefficient becomes dependent upon field strength (eq 1).

$$K(E) = K(0)[1 + \alpha(E/N)] \quad (1)$$

where *K*(0) is the mobility coefficient under low-field conditions and $\alpha(E/N)$ is an α function equal to $\alpha_2(E/N)^2 + \alpha_4(E/N)^4 +$ ..., where α_2, α_4, ... are specific coefficients of even powers of the electric field. Field dependence has been observed mostly for ions such as Li^+, Na^+, K^+, H^+, O_2^+, and CO^+ at subambient pressures.[4−7] The magnitude of the change in *K*(*E*) can be dramatic (∼80% increase between 3 and ∼180 Td for Li^+ in H_2) or negligible (∼10% increase between 2 and 200 Td for K^+ in N_2). In other instances, the mobility coefficient can decrease with field such as O_2^+ in O_2 (∼40% decrease from 2 to 500 Td).

Measurement of ion mobilities at atmospheric pressure beyond the low-field limit with conventional drift tubes is complicated by experimental considerations. For example, a power supply of 133.5 kV would be needed for a 5 cm long drift tube to reach an *E*/*N* of 100 Td (electric field of 26 700 V/cm at atmospheric pressure). During the past decade, an alternative design to characterize field-dependent mobilities of ions has been created using an asymmetric electric field between parallel plates with separations of 0.5 mm as shown in Figure 1.[8,9] Ions may be passed between these plates using gas flow and exposed to an electric field transverse to the ion path with magnitudes of ∼25 kV/cm ($E/N \approx 100$ Td) and frequencies of ∼1−2 MHz. Ions undergo displacement transverse to ion flow by an extent proportional to the differences in mobilities at high and low *E*/*N* and the duty cycle of the waveform (Figure 1). All ions, without intervention, are displaced with increasing number of cycles to the walls of the plates where collisional

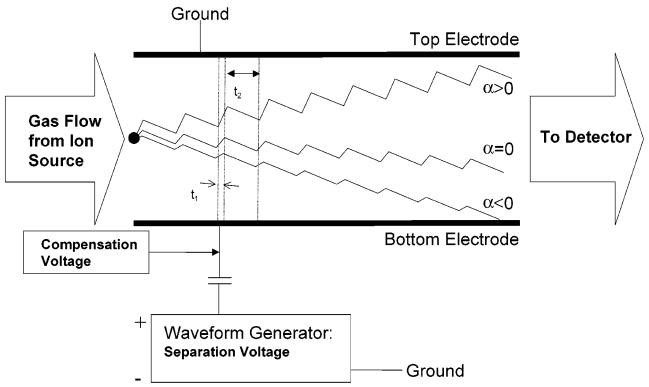

Figure 1. Schematic of planar field asymmetric ion mobility spectrometer. Ion paths are governed by the asymmetric electric field and field dependence of mobility for an ion.

10.1021/jp0221136 CCC: $25.00
Published on Web 04/16/2003

TABLE 1: Compensation Voltages for Several Separating Voltages for Moisture of 6.5 ppm for the Protonated Monomers of Organophosphorus Compounds

		separating voltages				
name	formula	1050 V	1150 V	1250 V	1350 V	1450 V
reactant ion peak	$H^+(H_2O)_n$	−10.95	−14.02	−17.96		
dimethylmethyl phosphonate (DMMP)	$C_3H_9O_3PH^+$	−3.95	−4.83	−5.40	−5.66	−5.86
trimethyl phosphate (TMP)	$C_3H_9O_4PH^+$	−3.65	−4.37	−4.90	−5.11	−5.12
diethylmethyl phosphonate (DEMP)	$C_5H_{13}O_3PH^+$	−2.53	−2.89	−3.07	−3.03	−2.78
diethylethyl phosphonate (DEEP)	$C_6H_{15}O_3PH^+$	−1.21	−1.32	−1.19	−0.81	−0.26
diisoprophylmethyl phosphonate (DIMP)	$C_7H_{17}O_3PH^+$	−2.19	−2.48	−2.52	−2.31	−1.97
diethylisoprophyl phosphonate (DEIP)	$C_7H_{17}O_3PH^+$	−1.69	−1.78	−1.69	−1.34	−0.87
triethyl phosphate (TEP)	$C_6H_{15}O_4PH^+$	−1.90	−1.98	−1.95	−1.65	−1.19
tripropyl phosphate (TPP)	$C_9H_{21}O_4PH^+$	−0.32	−0.70	−0.44	−0.09	0.48
dibutylbutyl phosphonate (DBBP)	$C_{12}H_{27}O_3PH^+$	−0.16	−0.11	0.20	0.80	1.56
tri-*n*-butyl phosphate (TBP)	$C_{12}H_{27}O_4PH^+$	−0.14	−0.02	0.31	1.03	1.45

neutralization occurs. However, a dc voltage or compensation voltage can be superimposed on the ac field and used to restore ions, in opposition to displacement by the ac field, for passage between the plates. Field dependencies of ions (the α function in eq 1) can be extracted from plots of ac amplitude versus the compensation voltage as shown for amines and amino acids.[10,11] The α functions or α(*E*/*N*) for a homologous series of normal ketones from acetone to decanone (M = C_3H_6O to $C_{10}H_{20}O$) were obtained in purified air with low moisture (~1 ppm_v)[12] using a planar, micromachined, high-field asymmetric ion mobility spectrometer (IMS).[13] Slopes of α(*E*/*N*) versus *E*/*N* for protonated monomers [$(MH^+(H_2O)_n$] were monotonic from 0 to 90 Td for acetone, butanone, and pentanone. However, plots of hexanone to octanone exhibited plateaus and plots for nonanone to decanone showed inversion above 70 Td. Slopes of α(*E*/*N*) versus *E*/*N* for proton-bound dimers [$M_2H^+(H_2O)_n$] for ketones with carbon numbers greater than five exhibited slopes that decreased continuously with increasing *E*/*N*.

Although there is no accepted model for field dependence of mobilities for large organic ions at atmospheric pressure, the positive α functions from protonated monomers of the homologous series of ketones were associated with collision cross sections for ion−molecule interactions.[12] If declustering of ions at high *E*/*N* is partly responsible for the field dependence, polar neutrals such as water should influence α functions. This has never been described in field-dependent studies with organic ions in air at atmospheric pressure. Because interests in the present work are restricted to large organic ions, a chemical class was needed in which ions at ambient pressure are not prone to fragmenting, to undergoing secondary reactions, or to exchanging charge through unfavorable reactions. Based on these criteria, the favored chemicals were organophosphorus compounds. These had an additional benefit of variations in mass and structure in the general form of $R'R_2P{=}O$ where R and R′ were alkyl groups (organophosphates) or where R′ was an alkyoxy group (organophosphonates). The objective of this work was to explore the effects of moisture on α(*E*/*N*) versus *E*/*N* for protonated monomers and proton-bound dimers of homologous series of organophosphorus compounds in air at atmospheric pressure and to refine a preliminary model for the field dependence of mobilities for large organic ions.[12]

Experimental Section

Instrumentation. Studies were completed using two independent and functionally identical planar micromachined drift tubes with field asymmetric waveform ion mobility spectrometry.[12,13] One drift tube was equipped with a gas chromatographic inlet to minimize the role of interferences in measurements and was used to obtain mobility scans for studies on field dependence of mobility.[14] A second drift tube was interfaced to a mass spectrometer for identification of the core ions from peaks in mobility scans.[15] The drift tubes in both instruments were identical in size and shape to those already described.[12−15] A distance of 0.5 mm was used for the gap between the electrodes. The drift tubes were operated using specialized electronics containing a radio frequency (RF) waveform generator, a sweeping voltage generator, and an electrometer. The waveform generator was based on a soft-switched, semiresonant circuit that incorporated a flyback transformer and allowed variable peak-to-peak amplitudes of the asymmetric waveform without altering the waveform shape (i.e., $f(t)$ is constant).[16] The operating frequency of the RF generator was 1.5 MHz, and the maximum amplitude was 1500 V. A compensation voltage ramp was synchronized with data collection and provided a scan of compensation voltage from −30 to +10 V at a frequency of 1 Hz. The complete analyzer was housed in an aluminum box approximately 12 × 10 × 5 cm^3. Signal was processed using a National Instruments board (model 6024E) to digitize and store spectra for every scan. The drift tube temperature was 60 °C. The ion source was ~2 mCi of ^{63}Ni. Air was provided at 1 L/min using a pure air generator (model 737, Addco Corp, Miami, FL) and was further purified through beds of activated charcoal and 13× molecular sieve. The moisture was measured by a Moisture Image Series 2 (Panametrics, Waltham, MA) and was nominally 0.1 ppm. Further control of moisture was accomplished by passing purified air though a chamber containing water and blending streams of dry and moist air.

The gas chromatograph was a Hewlett-Packard model 5880 equipped with a split/splitless injector and a 30 m RTX-50 capillary column (Supelco, Bellefonte, PA). Conditions of operation included the following: initial temperature, 100 °C; initial time, 0 min; temperature ramp, 10 °C/min; final temperature, 250 °C; final time, 10 min. The split ratio for the injector was 200:1, and injector temperature was 250 °C. Carrier gas was nitrogen at 2 mL/min. The mass spectrometer (MS) was tandem mass spectrometer (TAGA 6000, Sciex, Inc. Toronto, Ontario, Canada) with a 100 μm pinhole orifice to sample ions at ambient pressure. When the drift tube was placed against the flange of the MS, a hole in the drift tube was aligned with the pinhole in the flange of the MS.[15] The MS was equipped with an Apple PowerMac 7100/66 computer and API Standard Software, version 2.5.1.

Chemicals and Reagents. Ten chosen organophosphorus compounds (see Table 1) were obtained from various manufacturers in highest available purity. Stock solutions were prepared as mixtures of the organophosphorus compound in methylene chloride by diluting 1 μL of each chemical with solvent into 1000 μL of solution. A working solution was

prepared by combining 40 μL of every stock solution and diluting in 800 μL of methylene chloride. The concentration per compound in the working solution was ~300 ng/μL. Retention times were determined for individual chemicals prior to any studies, and chromatographic resolution was sufficient so that each compound could be characterized individually without interferences from other compounds. No detectable interferences were observed in these studies.

Procedures. In all studies of field dependence, 10 μL of the working solution was injected with a split so that 16 ng per compound were delivered to the GC column. This mass was provided to the drift tube in a near-Gaussian-shaped peak with width of 15 s. During sample collection, the analyzer was operated continuously and mobility scans were obtained every second. The maximum voltage of the asymmetric waveform was varied in six steps from 900 to 1500 V to obtain α functions.[12] Moisture in the drift gas was varied in 10 steps from 0.1 to 15 000 ppm by blending dried air (0.1 ppm moisture) with wet air (15 000 ppm moisture). Flows were controlled and blended in 10 combinations with a constant total flow of air at stable moisture levels.

Ion identification of a peak in a mobility scan was made in drift tube−MS experiments by setting the compensation voltage to pass ions from a single mobility peak to the MS. In these measurements, an individual neat chemical was placed in a vapor generator and headspace vapors were diluted and split to the drift tube. The vapor generator was a hermetically sealed glass container (200 mL), which was thermostated in an aluminum block equipped with a model 137 controller (Minco Products, Inc., Minneapolis, MN). Glass diffusion tubes or Teflon permeation tubes were placed in the glass container at temperatures from 35 °C for DMMP to 80 °C for TBP. All supply lines from the vapor generator to the drift tube were at 60 °C or more to minimize wall-adsorption by sample. This flow system allowed a constant gas flow to be delivered to the drift tube and permitted changes in vapor concentration by adjusting either the ratio of sample to diluent flows or the sample temperature. The diffusion or permeation tubes were weighed over time to determine gravimetrically concentrations in the sample flow (~5 μg/m^3).

Results and Discussion

Ionization Chemistry and Ion Separation by Field Asymmetric Ion Mobility Spectrometry. A scan of the compensation voltage for a drift tube with purified air at atmospheric pressure with a ^{63}Ni ion source produced a single intense peak in the mobility scan at ambient temperature and moisture of ~6.5 ppm$_v$. This peak appeared at a compensation voltage of −14.0 V dc with a separating voltage of 1150 V (field of 23 000 V/cm). This peak was isolated and passed to the IMS/MS where a mass spectrum was obtained with *m*/*z* values of 19, 37, 55, and 73 amu; these ions were identified as $H^+(H_2O)_n$ where $n = 1$ to 4, and the spectrum showed that the peak was a mixture of hydrated proton clusters. The quantitative composition of the peak was not determined owing to clustering and declustering reactions in the MS interface region between ambient pressure (660 Torr) and high vacuum (2×10^{-6} Torr). In addition, the mass spectra cannot accurately account for short-lived ion clusters such as $H^+(H_2O)_n(N_2)_n$, which may exist at ambient pressure in the drift tube but are altered in the supersonic jet expansion region of the IMS/MS. Hydrated protons are the predominant ions in positive polarity with purified air at ambient pressure, and the results here are consistent with such prior findings in ion mobility spectrometry.[17] The compensation voltage for this peak of hydrated protons was dependent upon the separation voltage as shown in Table 1, although ion displacement at high voltages (1350 and 1450 V) exceeded the capability of electronics to restore ions to stable passage through the drift tube.

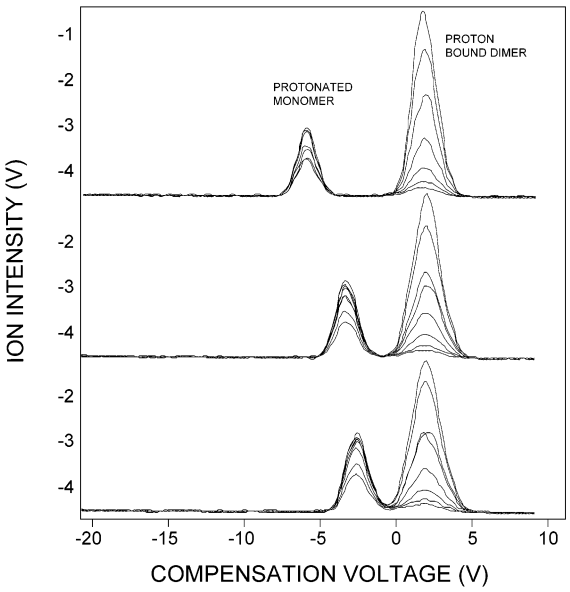

Figure 2. Mobility scans with field asymmetric ion mobility spectrometer for DMMP (top), DEMP (middle), and DIMP (bottom). Conditions were air at ambient pressure, moisture of 6.5 ppm$_v$, and separation voltage of 1350 V.

When vapors of an organophosphorus compound were added to gas flow of the drift tube, the intensity of the peak for $H^+(H_2O)_n$ declined and two other peaks appeared in the mobility scans. The abundances of these two peaks were governed by concentration of the compound in the vapor stream as shown in Figure 2 in which multiple scans are overlaid for DMMP, DEMP, and DIMP at several concentrations. Ions of the peak at compensation voltages of −6.5 V for DMMP (Figure 2, top frame) were introduced into the mass spectrometer of the IMS/MS by restricting the scan range for the compensation voltage to a single or narrow value centered on the peak maximum. The mass spectrum for this peak is shown in Figure 3 (top frame) and was comprised of a dominant ion at *m*/*z* of 125 amu. This was identified as the protonated monomer of DMMP, that is, $MH^+(H_2O)_n$ where M = $C_3H_9O_3P$ and $n = 0$. An ion at low intensity was observed at *m*/*z* 249, and this was identified as the proton-bound dimer of DMMP, that is, $M_2H^+(H_2O)_n$ where $n = 0$. This ion was formed through clustering of the protonated monomer with residual neutral DMMP in the gas flow through the drift tube. Low levels of neutrals of DMMP existed in the drift gas of this drift tube design (where ions and neutrals flow together through the analyzer) and could be drawn into the vacuum chamber of the MS. Very low amounts of hydrated protonated monomer ($MH^+(H_2O)_n$ where $n = 1$) at *m*/*z* of 143 amu could be seen in the mass spectrum with an expanded scale for abundance suggesting the existence of hydrated ions even at low moisture of ~1 ppm$_v$. Few quantitative conclusions should be made from these results owing to the complexity of ion clustering and declustering from the interface between atmospheric pressure and high vacuum.[18] The importance of these figures is only that the core ion can be identified. The peak at +1 V in Figure 2 (top frame) was also isolated and mass-identified yielding Figure 3 (bottom frame). The predominant ion was the proton-bound dimer at *m*/*z* 249, that is, $M_2H^+(H_2O)_n$ where $n = 0$, and this result was consistent with prior

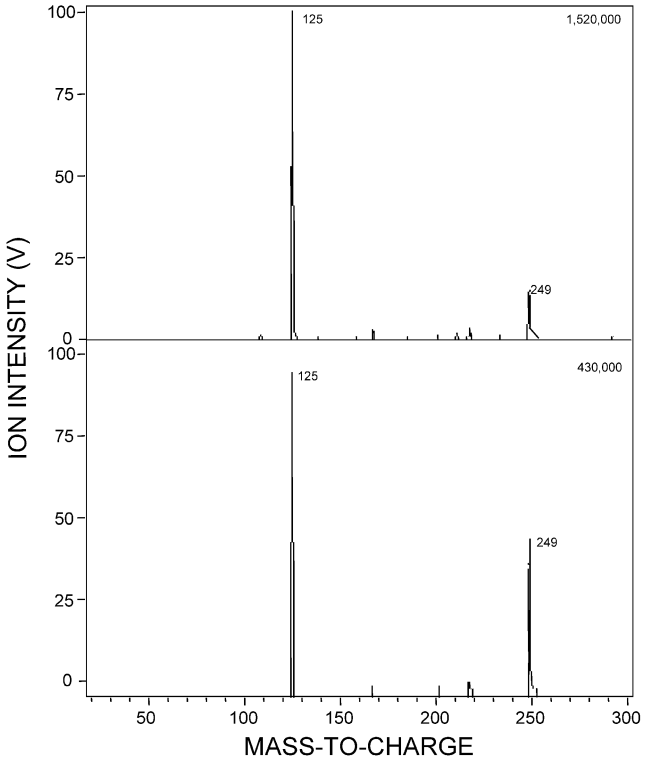

Figure 3. Mass spectra for peaks in mobility scans for DMMP. A mass spectrum (top frame) was obtained for the peak at +2 V compensation voltage, and a mass spectrum (bottom frame) was obtained for the peak at −6.6 V compensation voltage.

patterns in compensation voltages for peaks with a homologous series of ketones.[12] The other major ion at *m*/*z* 125 amu was the protonated monomer and was understood to have formed in the interface region between the IMS and MS as the proton-bound dimer was partially decomposed in the transition between ambient pressure and high vacuum. Control of MS lens potentials demonstrated that the ratio of proton-bound dimer to protonated monomer could be controlled by lens potentials.[18] No other ions of significant intensity were observed, and the core ion was assigned to a proton-bound dimer. This pattern of protonated monomer and proton-bound dimer was observed for all other organophosphorus compounds of Table 1 through ion identification with IMS/MS.

Compensation Voltage and α Functions for Organophosphorus Compounds. The compensation voltages for the protonated monomers and proton-bound dimers were dependent upon the magnitude of the separation voltage applied to the drift tube, and this dependence for protonated monomers is shown for all chemicals in Table 1. As the separation voltage was increased, the compensation voltages needed to pass ions through the drift tube changed. The trend in these dependencies can be seen for protonated monomer in Table 1 and in Figure 4 for 6.5 ppm moisture in air. The influence of separation voltage amplitude (*S*) on compensation voltage (*C*) is dependent on the α function of an ion (see eq 1). The general trend in plots with increased separation voltage was the movement of *C* for proton-bound dimers toward positive potentials and the movement of *C* for protonated monomers toward negative potentials with slight inversion in slope above 1400 V (field 28 000 V/cm).

The α functions were extracted from plots of compensation voltage versus separation voltage using methods described previously[12] and are shown as plots of α versus *E*/*N* in Figure 5 for all organophosphorus compounds at 6.5 ppm moisture in

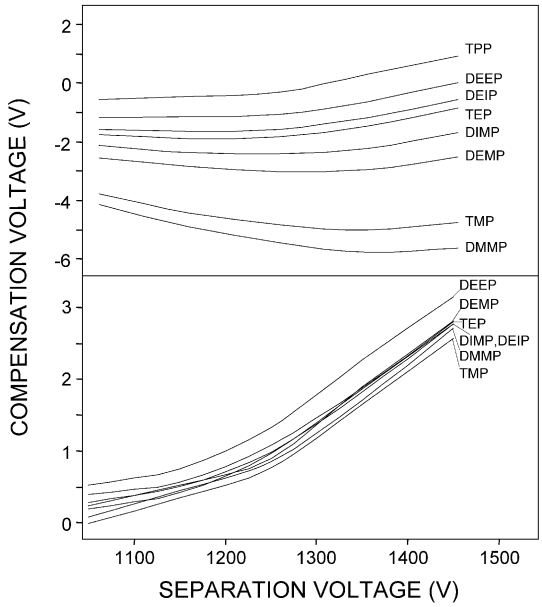

Figure 4. Plots of compensation voltage versus separation voltage with moisture of 6.5 ppm_v. Top frame is for protonated monomers, and bottom frame is for proton-bound dimers. Abbreviations can be found in Table 1.

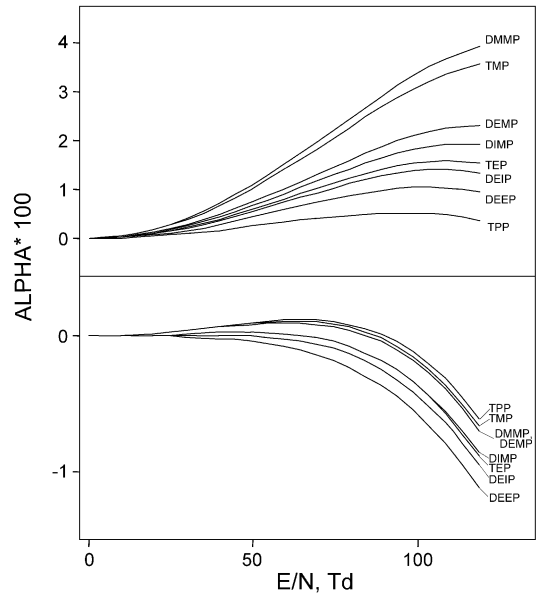

Figure 5. Plots of α functions at 6.5 ppm_v moisture in air at atmospheric pressure. Top frame is for protonated monomers and bottom frame is for proton-bound dimers.

air. Numerical results from these determinations are summarized in Table 2 in which measurement variance is also shown and is regarded as inconsequential to the determinations. These plots are fundamental features of ions because the α function is independent of the drift tube dimensions. Certain general tendencies can be seen in the α functions for organophosphorus compounds as shown in Figure 5. These include the following: (A) the α values correlate with inverse ion mass; (B) a few ions are exceptions to these trends, and different α functions are exhibited by DIMP, DEIP, and TEP though common in mass (suggesting a structure dependence in α functions); (C) DEEP is another exception in which a low mass also shows a comparatively low α; (D) the resolution between protonated monomer and proton-bound dimer for DBBP and TBP is insufficient at moistures of 6.5 ppm to determine compensation

TABLE 2: Values of α[a] for Organophosphorus Compounds for Protonated Monomer and Proton-Bound Dimer at 6.5 ppm Moisture in Air at Atmospheric Pressure and Calculated Errors

protonated monomer	α_2	α_4	variance[b]
DMMP	5.093×10^{-6}	-1.58×10^{-10}	0.9997
TMP	4.756×10^{-6}	-1.554×10^{-10}	0.9985
DEMP	3.384×10^{-6}	-1.246×10^{-10}	0.9855
DEEP	1.928×10^{-6}	-9.384×10^{-11}	0.9949
DIMP	3.001×10^{-6}	-1.193×10^{-10}	0.9983
DEIP	2.419×10^{-6}	-1.087×10^{-10}	0.9937
TEP	2.641×10^{-6}	-1.148×10^{-10}	0.9938
TPP	1.278×10^{-6}	-7.72×10^{-11}	0.9908
DBBP	5.381×10^{-7}	-4.671×10^{-11}	0.9871
TBP	6.905×10^{-7}	-5.898×10^{-11}	0.9902
proton-bound dimer	α_2	α_4	variance[b]
DMMP	7.383×10^{-7}	-7.925×10^{-11}	0.9982
TMP	8.111×10^{-7}	-8.093×10^{-11}	0.9958
DEMP	6.198×10^{-7}	-7.53×10^{-11}	0.9927
DEEP	2.754×10^{-7}	-6.403×10^{-11}	0.9939
DIMP	5.418×10^{-7}	-7.055×10^{-11}	0.9976
DEIP	6.548×10^{-7}	-7.654×10^{-11}	0.9952
TEP	4.103×10^{-7}	-6.453×10^{-11}	0.9963

[a] Reference to eq 1. [b] Variance is derived from the difference between experimental points and fitted function for the dependence of *C* versus *S*.[12]

voltages of individual ions. Consequently, these two are absent from plots or determinations at low moistures.

The scale for α plots for a homologous series of ketones[12] was large compared to that for organophosphorus compounds as shown in Figure 5. For example, the α functions for the protonated monomers of acetone, butanone, and pentanone were ~0.1 in contrast to values of 0.01−0.04 for the organophosphorus compounds. This may be associated largely with mass because the α values for large ketones (octanone and decanone) were comparable to those for small organophosphorus compounds (DMMP, TMP, and DEMP) of similar ion mass. Shapes of the plots of α versus *E*/*N* between these two sets of chemicals are also comparable suggesting that mass alone makes a large contribution to the α functions. This is also consistent with plots for proton-bound dimers (Figure 5, bottom frame and Table 2) for which α values range between 0 and −0.01 for ions with masses from 251 to 451 amu though trends with mass are not proportional and do not mirror those for the protonated monomer (Figure 5, top frame). Proton-bound dimers for ketones with masses of 117−285 amu showed changes only between +0.02 and −0.05 suggesting again a mass dependence in the magnitude of α. Moreover, proton-bound dimers of ketones exhibited a proportional dependence on ion mass suggesting that the patterns for proton-bound dimers of organophosphorus compounds involve more than mass alone, for example, a contribution from a structural component.

Effects of Moisture on Ion Mobility. The influence of moisture on plots of compensation versus separation voltage and the α functions is shown for organophosphorus compounds at 9500 ppm_v moisture in Figures 6 and 7, respectively. These plots can be compared directly with results in Figures 3 and 4 for the same studies at 6.5 ppm. An immediate contrast is that the compensation voltage for protonated monomers at 9500 ppm_v moisture is dramatically different (−3 to −27 V) in comparison to those at 6.5 ppm_v moisture (0 to −4 V). Also, the range of compensation voltages is dramatically larger for the higher moisture atmosphere than for the low moisture one (−4 to −5 V). As an example, DMMP shows a compensation

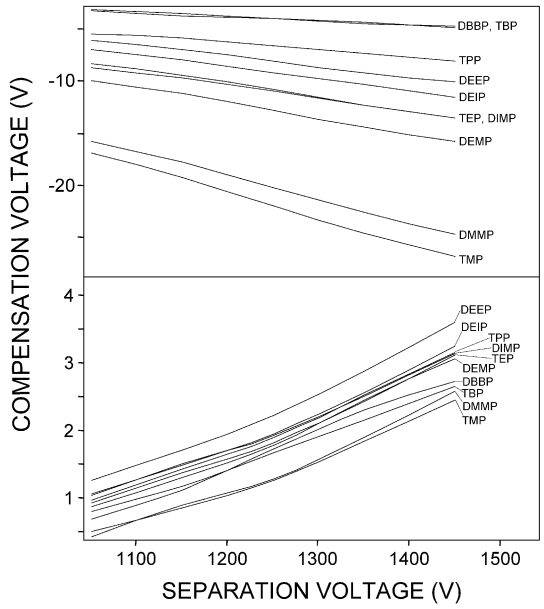

Figure 6. Plots of compensation voltage versus separation voltage with moisture in air of 9500 ppm_v. Top frame is for protonated monomers and bottom frame is for proton-bound dimers.

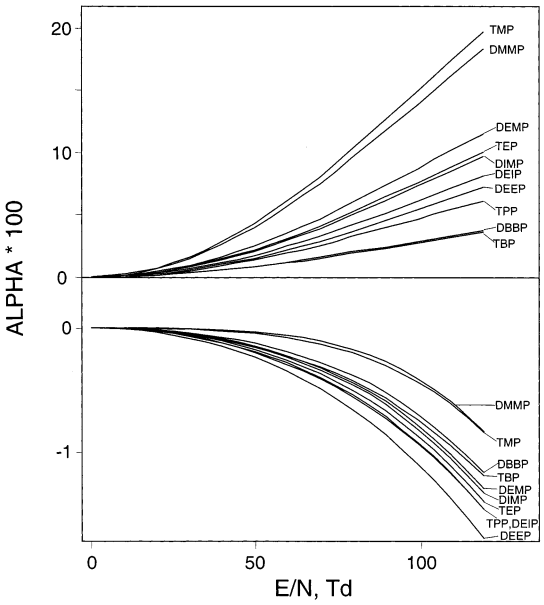

Figure 7. Plots of α functions at 9500 ppm_v moisture in air at atmospheric pressure. Top frame is for protonated monomers and bottom frame is for proton-bound dimers.

voltage from −15 to −22 V at 9500 ppm_v moisture for separation voltages between 1100 and 1400 V compared to −4 to −6 V at 6.5 ppm_v.

The effect of moisture (6.5 versus 9500 ppm_v) on the proton-bound dimer is comparatively minor in absolute voltage at low and high fields as shown in the bottom frames of Figures 4 and 6. Compensation voltages for peaks at low separation voltage are 0−0.5 V at 6.5 ppm_v moisture and 0.5−1.3 V at 9500 ppm_v moisture. Similarly, the ranges of change with separation voltages were comparable at 0−3 V and 0.5−3.2 V, respectively. This similarity in the α functions for proton-bound dimers is shown in comparisons of Figure 7 (bottom frame) and Figure 5 (bottom frame). Despite the general similarities, some noticeable differences can be observed for certain ions. The most remarkable differences were found with DBBP and TBP for

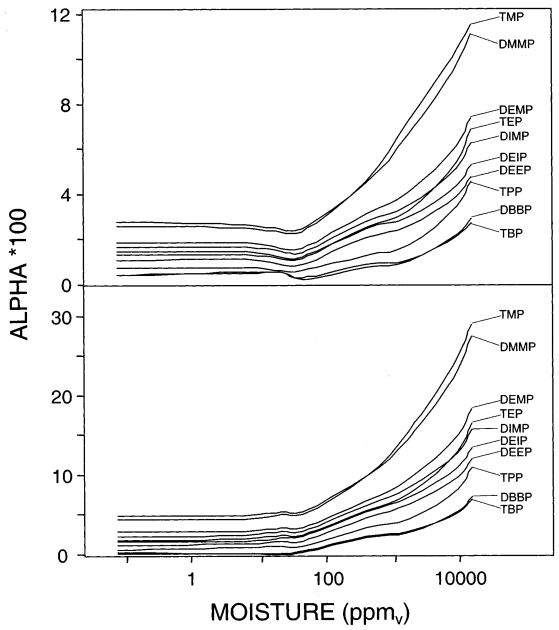

Figure 8. Plot of α versus moisture for protonated momers at two fields of 80 (bottom) and 140 (top) Td.

which protonated monomer and proton-bound dimer could be resolved at 9500 ppm_v moisture (Figure 7). At low moisture, these ions were not resolvable at any separation field but were separated at high moistures.

The effect of moisture on α functions for protonated monomers across a wide range from 0.1 to 10000 ppm_v is shown in Figure 8 for two settings of separation field (as *E*/*N*), 80 Td (bottom frame) and 140 Td (top frame). The patterns of dependence on moisture are comparable with both values of *E*/*N* although the magnitudes for α at 10 000 ppm_v differ at 80 and 140 Td by 0.02−0.11 and 0.05−0.28, respectively. For both values of *E*/*N*, the α function is nearly constant from 0.1 to ∼10 ppm_v moisture and is seen as level plots in Figure 8, and the influence of moisture is first evident between 10 and 100 ppm_v. The influence on α increases steadily between 100 and 10 000 ppm_v. Another pattern evident in Figure 8 is the relative response for α functions for all organophosphorus compounds. Nearly all compounds showed comparable slopes for the α function versus moisture except TMP and DMMP. These two were more affected by moisture than any other compound and also were the two lowest mass ions. This may be consistent with a nonlinear mass dependence of α function with moisture.

A topographic view of the dependence of α(*E*/*N*) on moisture and *E*/*N* is shown for protonated monomers of THP (top frame) and DEIP (bottom frame) in Figure 9. The results show that α was affected largely at moisture between 1000 and 10 000 ppm_v and *E*/*N* between 60 and 140 Td. Large regions of nearly stable response exist below 100 ppm_v moisture with all values of *E*/*N*. These plots provide a graphic summary of the conclusion from all other findings in this study: namely, dependence of α(*E*/*N*) on moisture in the drift gas of the mobility spectrometer is similar in appearance for protonated monomers for all organophosphorus compounds. Moisture did not influence the α values for dimer ions significantly as shown by the scale of response in Figures 5 and 7. Finally, an extrapolation of plots to zero moisture suggests that field dependence of mobility will exist at atmospheric pressure in absolutely dry air (i.e., mobility changes exist in air in the absence of water neutrals). This means that neutrals other than water are involved in the changes in mobility with field.

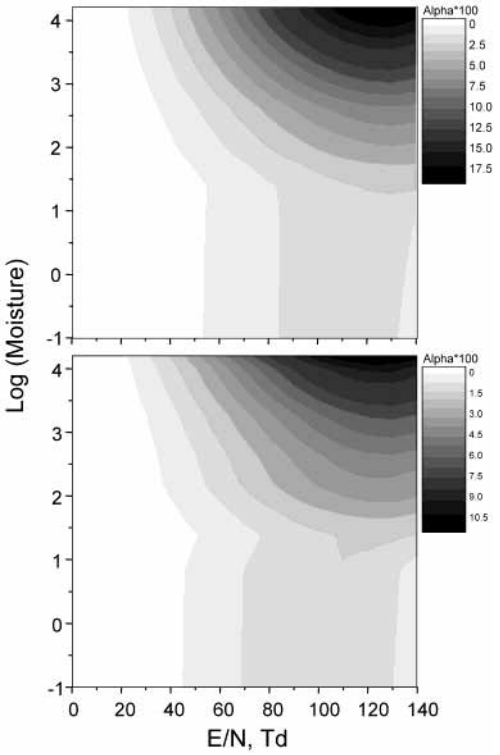

Figure 9. Topographic plots of α versus log (moisture) and field (*E*/*N*) for THP (top frame) and DEIP (bottom frame).

Model of Field Dependence. The dependencies of the α function on water content as shown in Figure 8 can be divided into two regions with a demarcation at ∼ 50 ppm. Below this value, α(*E*/*N*) is independent of water content but has a different value for each of the protonated phosphates and phosphonates. Above ∼50 ppm, α(*E*/*N*) increases monotonically for all ions. In both regions, for each ion, the difference in mobility between high- and low-field portions of the applied waveform may be ascribed to an increase in the mobility coefficient at high field arising from a decrease in the effective ion cross section. The cross section will be governed by the degree of solvation of the protonated molecule by neutral molecules. At high field, the more weakly held molecules will be removed as the effective temperature of the cluster ion increases, while at low field, solvation will increase as the effective temperature is lowered. The same desolvation and solvation will occur in each field cycle. The above explanation may be valid only if there is sufficient time during the low-field period for solvent molecules to encounter the ion. The explanation must be consistent with the 50 ppm demarcation region below which water has no effect on α.

At 50 ppm water in air at ambient temperature and pressure, there are 1.3×10^{15} molecules/cm^3. If the usual collision rate constant of $\sim 1 \times 10^{-9}$ cm^3/(molecule s) is taken for ion neutral encounters and with the knowledge that the concentration of ions is far less than that of water, then the time between collisions is approximately $1/(k[H_2O]) = 0.8$ μs. In the low-field period of ∼1.6 μs, an ion will encounter approximately two water molecules, a sufficient number, if the association reaction is efficient, to change the mass and the cross section of the ion. At higher water concentrations, the number of collisions in the low-field period will increase proportionately, 400 at 10 000 ppm. With an increase of water concentration, the potential cluster size will increase but the strength of the attachment of each succeeding water molecule will decrease. The larger clusters will be more susceptible to size diminution

in the same high field than are the smaller ones, and hence, the value of α will increase with increasing water concentration. Consistent with this picture is the difference in the α values shown in Figure 8 when the high field is changed and the low field remains the same. The larger field leads to a greater extent of declustering, but the extent of clustering at low field, dependent on time and water concentration, remains the same. The result is an increase in α by approximately a factor of 4 when the high portion of the field is changed from 80 to 140 Td. It is to be noted that with both values of the high field the lower mass ions show the greatest changes in the values of α as the water concentration is increased. For the ions in this study, lower mass also implies a smaller ion the cross section of which will change to a greater extent than will that of a larger ion by the addition of the same number of water molecules.

Below ~50 ppm water, a change in concentration has no effect on the value of α for any of the ions. We interpret this to mean that the degree of hydration of the ions is not changed from high to low field. There are at least two explanations for this: (a) the ions are not hydrated; (b) the ions are hydrated but the few attached water molecules are so tightly bound that they cannot be removed by the high field and there is no opportunity for water attachment during the low-field period due a negligible number of ion/molecule collisions. We have no means of deciding between the two possibilities.

There is an increase in α for each ion below 50 ppm water when the high field is increased. Figure 8 shows a change of a factor of 2. If this change is also due to a change in ion solvation between high and low field, then the solvating molecule must be either an unknown impurity in the air drift gas or the air drift gas itself. This latter conjecture is consistent with a recent study of the effect of carrier gas type on the high- to low-field mobility of several types of ions.[20] The nitrogen molecule with no dipole moment and a very low polarizability (1.74×10^{-24} cm^3) is a very poor solvent compared with water for gas-phase ions. There are very few quantitative studies of N_2 as a gas-phase solvent with which to make comparisons. One example for which data are available is the solvation of NO^+. The values (kJ mol^{-1}) of the enthalpy changes for the addition of the first three solvent molecules are as follows: for H_2O, 95.0, 67.4, and 23;[21] for N_2, 19, 17, and 16.[22] However, because an ion will experience a collision with a nitrogen molecule of the drift gas roughly once every 40 ps, an equilibrium solvation can occur in the low-field period. The difference of the factor of 2 in the α value for the two high fields implies that solvation by nitrogen can also occur at high field, but the extent is reduced with increase of field strength.

Conclusions

The dependence of mobility on *E*/*N* and the influence of moisture provided an insight into the source of positive slopes for α, the function that describes the field dependence for a particular ion. The field dependence for protonated organo-phosphorus monomers, which are susceptible to the formation of hydrated ions, was noticeably affected by moisture and could be understood to arise from increased hydration numbers of the ion $MH^+(H_2O)_n$, that is, the most loosely bound water adducts only at moisture levels above 50 ppm_v. The proton-bound dimers in contrast are not significantly hydrated and did not exhibit positive ion dependence. At levels of moisture below 50 ppm_v, the kinetics of forming ion clusters with water are too slow for a cluster to form during the low-field portion of the waveform applied to the drift tube. Consequently, clusters must arise from neutrals other than water, and field dependence of α should be found in many collisions of an ion with loosely held nitrogen neutrals.

Acknowledgment. Support is gratefully acknowledged through grants from NASA (Grant No. 00-HEDS-01-110) and from the US Army (Contract Nos. DAAM01-97-D-0006, D.O. 0002 GC-3173-RFP-02-005).

References and Notes

(1) Mason, E. A.; McDaniel, E. W. *Transport Properties of Ions in Gases*; John Wiley and Sons: New York, 1988, 266−326.
(2) Maitland, G. C. *Intermolecular forces: their origin and determination*; Clarendon Press: Oxford, U.K., 1987; p 616.
(3) McDaniel, E. W.; Cermak, V.; Dalgarno, A.; Ferguson, E. E.; Friedman, L. *Ion Molecule Reactions, Transport Properties of Ions in Gases*, John Wiley and Sons: New York, 1970; p 65.
(4) Ellis, H. W.; Pai, R. Y.; McDaniel, E. W.; Mason, E. A.; Viehland, L. A. *At. Data Nucl. Data Tables* **1976**, *17*, 177−210.
(5) Ellis, H. W.; McDaniel, E. W.; Albritton, D. L.; Viehland, L. A.; Lin, S. L.; Mason, E. A. *At. Data Nucl. Data Tables* **1978**, *22*, 179−217.
(6) Ellis, H. W.; Thackston, M. G.; McDaniel, E. W.; Mason, E. A. *At. Data Nucl. Data Tables* **1984**, *31*, 113−151.
(7) Viehland, L. A.; Mason, E. A. *At. Data Nucl. Data Tables* **1995**, 60, 37−95,.
(8) Buryakov, I. A.; Makas, A.; Krylov, E. V.; Nazarov, E. G.; Pervukhin, V. V.; Rasulev, U. Kh. *Soviet Technol. Phys. Lett.* **1991**, *17* (6), 60−65.
(9) Buryakov, I. A.; Krylov, E. V.; Nazarov, E. G.; Rasulev, U. Kh. *Int. J. Mass Spectrom.* **1993**, *128*, 143−148.
(10) Viehland, L. A.; Guevremont, R.; Purves, R. W.; Barnett, D. A. *Int. J. Mass Spectrom.* **2000**, *197*, 123.
(11) Guevremont, R.; Barnett, D. A.; Purves, R. W.; Viehland, L. A. *J. Chem. Phys.* **2001**, *14* (3), 10270−10277.
(12) Krylov, E.; Nazarov, E. G.; Miller, R. A.; Tadjikov, B.; Eiceman, G. A. *J. Phys. Chem. A* **2002**, *106*, 5437−5444.
(13) Miller, R. A.; Eiceman, G. A.; Nazarov, E. G.; King, A. T. *Sens. Actuators, B* **2000**, *67*, 300−306.
(14) Eiceman, G. A.; Nazarov, E. G.; Miller, R. A.; Krylov, E.; Zapata, A. *Analyst* **2002**, *127* (4), 466−471.
(15) Eiceman, G. A.; Nazarov, E. G.; Miller, R. A. *Int. J. Ion Mobility Spectrom*. **2001**, *3*, 15−27.
(16) Krylov, E. V. *Instrum. Exp. Tech*. **1997**, *40*, 628−632.
(17) Kim, S. H.; Betty, K. R.; Karasek, F. W. *Anal. Chem.* **1978**, *50* (14), 2006−2011.
(18) Wensing, M. W.; Snyder, A. P.; Harden, C. S. *Rapid Commun. Mass Spectrom*. **1996**, *10* (10), 1259−1265.
(19) Rayleigh, L. *Proc. R. Soc. London* **1900**, *66*, 68−74.
(20) Barnett, D. A.; Ells, B.; Guevremont, R.; Purves, R. W.; Viehland, L. A. *J. Am. Soc. Mass Spectrom.* **2000**, *11*, 1125−1133.
(21) French, M. A.; Hills, L. P.; Kebarle, P. *Can. J. Chem.* **1973**, *51*, 456−461.
(22) Hiraoka, K.; Yamabe, S. *J. Chem. Phys.* **1989**, *90*, 3268−3273.